

# Local dynamics and phase transition in quantum paraelectric SrTiO<sub>3</sub> studied by Ti *K*-edge x-ray absorption spectroscopy

Andris Anspoks<sup>1</sup>, Janis Timoshenko<sup>1</sup>, Juris Purans<sup>1</sup>, Francesco Rocca<sup>2</sup>, Vladimir Trepakov<sup>3,4</sup>, Alexander Dejneka<sup>4</sup> and Mitsuru Itoh<sup>5</sup>

<sup>1</sup> Institute of Solid State Physics, University of Latvia

<sup>2</sup> IFN-CNR, Institute for Photonics and Nanotechnologies, Unit FBK-Photonics, Trento, Italy

<sup>3</sup> Institute of Physics, AS CR, Prague, Czech Republic

<sup>4</sup> Ioffe Physical-Technical Institute RAS, St-Petersburg, Russia

<sup>5</sup> Tokyo Institute of Technology, Japan

E-mail: andris.anspoks@cfi.lu.lv

**Abstract.** Strontium titanate is a model quantum paraelectric in which, in the region of dominating quantum statistics, the ferroelectric instability is inhibited due to nearly complete compensation of the harmonic contribution into ferroelectric soft mode frequency by the zero-point motion contribution. The enhancement of atomic masses by the substitution of <sup>16</sup>O with <sup>18</sup>O decreases the zero-point atomic motion, and low-T ferroelectricity in SrTi<sup>18</sup>O<sub>3</sub> is realized. In this study we report on the local structure of Ti in SrTi<sup>16</sup>O<sub>3</sub> and SrTi<sup>18</sup>O<sub>3</sub> investigated by Extended X-ray Absorption Fine Structure measurements in the temperature range 6 – 300 K.

## 1. Introduction

Strontium titanate (SrTiO<sub>3</sub>, STO) is a well-known and thoroughly studied member of the family of ABO<sub>3</sub> oxides, which at room temperature has the cubic *Pm3m* perovskite-type structure. Upon cooling, STO undergoes a second order *Pm3m* to *I4/mcm* antiferrodistorsive (AFD) phase transition (PT) at  $T_C = 105$  K, with condensation of the  $R_{25}$  phonon mode at the Brillouin zone boundary [1]. STO is called quantum paraelectric [2] because at low temperatures, where quantum statistics dominates, the ferroelectric ordering is suppressed and the rising of dielectric permittivity saturates. This leads to the idea that ferroelectricity in STO can be induced by suppression of the quantum fluctuations. Experimentally, this was observed using isotope exchange (<sup>16</sup>O with <sup>18</sup>O) [3, 4].

The long debate about the structure of the polar phase and the mechanism of the phase transition in SrTi<sup>18</sup>O<sub>3</sub> is still open [4, 5]. The structure of STO has been studied by different experiments as X-ray diffraction (XRD) [6], neutron diffraction [7] and X-ray absorption spectroscopy [8, 9], but a clear picture and consistence of opinions have not yet been achieved.

In this work the local atomic structure around Ti in SrTi<sup>16</sup>O<sub>3</sub> (STO16) and SrTi<sup>18</sup>O<sub>3</sub> (STO18) is studied in the temperature range 6 – 300 K with x-ray absorption spectroscopy methods, namely Extended x-ray Absorption Fine Structure (EXAFS), using radial distribution function reconstruction [10] and advanced Reverse Monte Carlo (RMC) and Evolutionary Algorithm (EA) techniques for EXAFS data analysis (RMC/EA-EXAFS) [11].



## 2. Samples and experiment

In our study we used powders of standard STO16 and STO18 where 96 % of oxygen atoms were substituted by  $^{18}\text{O}$  as described in [4].

The Ti K-edge x-ray absorption spectra were measured in transmission mode at the ESRF bending-magnet beamline BM23 and at the HASYLAB/DESY A1 bending-magnet beamline in the temperature range from 6 K to 300 K. The x-ray radiation was monochromatized by a 40 % detuned Si(111) double-crystal monochromator, and the beam intensity was measured using two ionization chambers filled with argon and krypton gases. The Oxford Instruments liquid helium flow cryostat was used to maintain the required sample temperature. To achieve the best sample homogeneity and thickness at the Ti K-edge, necessary for transmission mode experiments, the proper amount of the STO powder was deposited on polytetrafluoroethylene Millipore membranes from suspensions in methyl alcohol.

## 3. Results

The extended x-ray absorption fine structure (EXAFS) oscillations  $\chi(k)$  and X-ray absorption near edge structure (XANES) data were extracted following the conventional procedure [12, 13] using the EDA software package [14]. The theoretical spectra, scattering amplitudes and phase shift functions were calculated by ab initio real-space multiple-scattering code FEFF8.5 [15] using the complex exchange-correlation Hedin-Lundqvist potential in the muffin-tin (MT) self-consistent-field approximation with the default values of MT radii.

First results and analyses including detailed studies of the x-ray absorption near edge structure (XANES) pre-peak structure [16] show that spectra of STO18 and STO16 look very similar because the difference in the structure between STO18 and STO16 is very small [3]. XANES analysis was done on the second pre-peak ("B"), because its intensity is proportional to the squared displacement of the Ti [17]. This peak is originating from transitions of Ti 1s electron to the p-d hybrid orbitals (titanium 3d orbital mixing with the oxygen 2p orbitals due to the Ti displacement from the center of the octahedra) [17]. Our data [16] revealed noticeable anomaly of the temperature dependence for STO18 pre-peak "B" intensity in the low temperature region: STO18 has higher intensity of the pre-peak "B" than STO16. Normally one should expect the opposite: that with the increase of the oxygen mass the oscillation amplitudes should decrease.

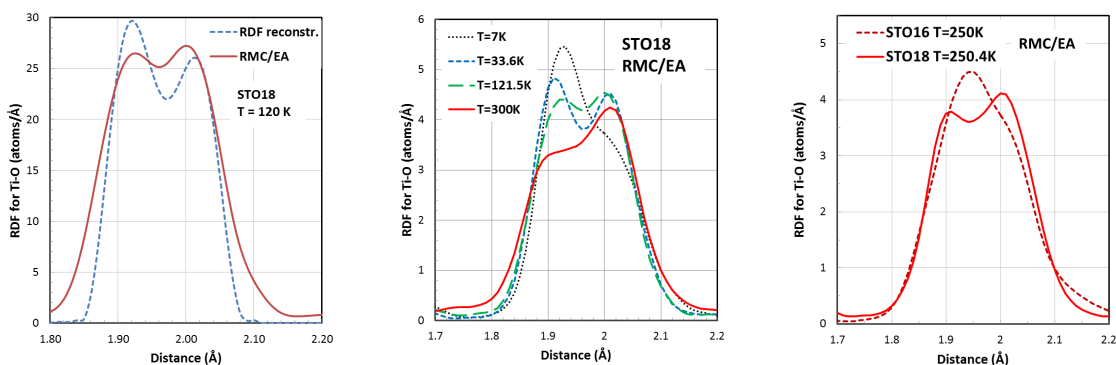


**Figure 1.** RDF for the first coordination shell of Ti ( $\text{Ti-O}_1$ ).

### 3.1. Radial distribution function (RDF) reconstruction method

As next step we started with the analysis for the first coordination shell  $\text{Ti-O}_1$  using a model-independent approach [10], which allowed one to reconstruct the true radial distribution function (RDF). The Ti  $K$ -edge EXAFS contribution  $\chi(k)k^2$  for the first coordination shell was isolated

using Fourier filtering procedure and best-fitted in  $3 - 16 \text{ \AA}^{-1}$  of the k-space using EDARDF code [14]. The obtained results (left panel of figure 1) show a clear non-Gaussian character of the RDFs for the first coordination shell of Ti even for  $T = 120 \text{ K}$  which is a cubic phase according to the crystallographic data.

### 3.2. RDF analysis from RMC/EA method

To reveal the local atomic structure beyond the first coordination shell we applied our newly developed reverse Monte Carlo (RMC) and evolutionary algorithm (EA) technique for EXAFS data analysis (RMC/EA-EAXFS) [11]. The method does not restrict the geometry of the system and takes into account all multiple scattering effects, which are very sensitive to the bonding angles and distances, e.g. in Ti-O-Ti chains and triangles.

In the presented RMC/EA-EXAFS simulations we used a set of 128 supercells, where each supercell has size  $4a \times 4b \times 4c$  and contains 1280 atoms. Lattice constants  $a$ ,  $b$  and  $c$  and initial positions of the atoms were taken from diffraction studies [7]. Comparison of the experimental and theoretical EXAFS spectra has been performed using a Morlet wavelet transform (WT) [18] in  $3 - 16 \text{ \AA}^{-1}$  of the k-space, and  $0.9 - 4.5 \text{ \AA}$  of the R-space range. The WT allows one to obtain a two-dimensional representation of the periodic signal with simultaneous localization in k and R spaces, WT allows to better separate the contribution to the total EXAFS from the noise due to imperfections in background subtraction procedure [18]. Scattering paths with the half-path length up to  $5.5 \text{ \AA}$  and the multiple-scattering contributions up to the third order were considered in our simulations. The calculation of the cluster potential was performed only once for the average atom configuration, corresponding to the STO crystallographic structure. The complex exchange-correlation Hedin-Lundqvist potential and default values of muffin-tin radii, as provided within the FEFF8.5 code [15], were employed. As the output of RMC/EA-EXAFS analysis we have obtained a set of atomic coordinates, which can be used to calculate RDF, average distance between atoms, mean-square relative displacement (MSRD), and other values. MSRD values here are calculated as the second moment for the corresponding path.

The obtained RDFs for Ti-O<sub>1</sub> (figure 1) are consistent with the RDF reconstruction method and confirm the non-Gaussian character of the RDFs. We have found that there are two well resolved groups of oxygen atoms separated by  $\sim 0.1 \text{ \AA}$  in the first coordination shell of Ti in STO18, in the whole range of investigated temperatures (figure 1). The same applies to STO16, but the corresponding distance between two groups of oxygen atoms is smaller. The variations of the amplitudes seen in figure 1 most probably are due to the too low statistics, because they vary with the changes of the simulation parameters. At the same time, in all simulations there are two well resolved groups of oxygen atoms.

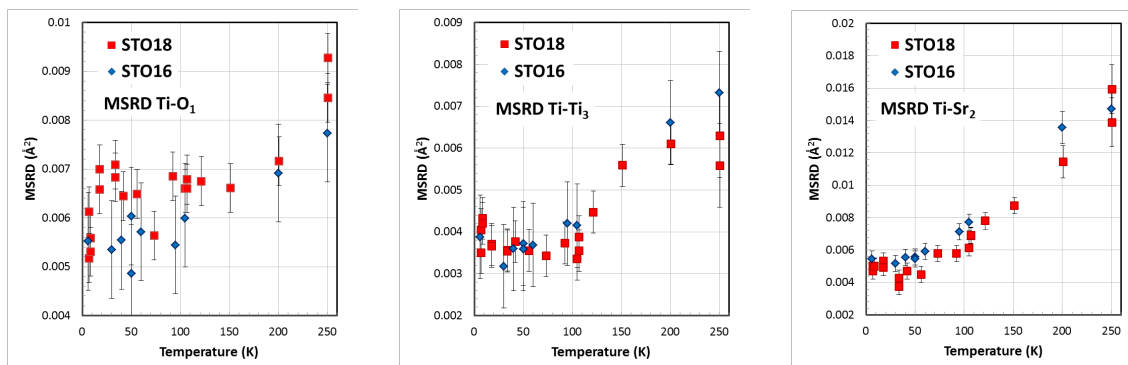


**Figure 2.** MSRD values obtained with RMC/EA-EXAFS for Ti-O<sub>1</sub>, Ti-Sr<sub>2</sub>, and Ti-Ti<sub>3</sub>.

### 3.3. MSRD analysis from RMC/EA method

The absolute values of MSRD for the first coordination shell of Ti (Ti–O) (left panel of figure 2) in the low temperature region for STO18 are larger than those for STO16 which is in-line with XANES analysis results. Normally one should expect opposite effect where with the increase of the oxygen mass the MSRD values should decrease as it was observed in the case of germanium [19].

The MSRD values for the first coordination shell of Ti in STO18 have an anomaly in the vicinity of the low-T phase transition into polar phase (25 K).

There is a strong correlation between nearest neighboring Ti atoms for STO in the whole range of the temperatures, as shown by the low MSRD value for Ti third coordination shell (Ti–Ti) (middle panel of figure 2). At the same time, Ti–Ti MSRD values show a noticeable increase around AFD PT in the 105 – 150 K region.

MSRD values for the second coordination shell of Ti (Ti–Sr) (right panel of figure 2) have the strongest temperature dependence, with standard Einstein-like temperature behavior in the high temperature region, corresponding to the paraelectric phase. Ti–Sr MSRD for STO18 shows a jump-like discontinuity at 25 K where the MSRD value increases going to lower T. No anomalies are observed for Ti–Sr MSRD for STO16 in the low temperature region.

The nature of the observed effects can be static or dynamic. It is important to note that our measurements revealed the presence of some static and dynamic disorders also in STO16, but less pronounced than in STO18. This can be connected to precursor effect widely discussed today [5].

### Acknowledgments

This work has been supported by the Latvian Science Council grant no. 402/2012. The work was supported in part from large infrastructure SAFMAT Project CZ.2.13/3.1.00/22132, P108/12/1941 of GACR. Authors wish to thank Dr. Olivier Mathon from ESRF and Dr. Edmund Welter from DESY for assistance during the beamtimes, and Dr. Alexei Kuzmin for fruitful discussions and feedback.

### References

- [1] Shirane G, and Yamada Y 1969 *Phys. Rev.* **177** 858–863
- [2] Muller K A and Burkard H 1979 *Phys. Rev. B* **19** 3593–3602
- [3] Itoh M, Wang R, Inaguma Y, Yamaguchi T, Shan Y-J and Nakamura T 1999 *Phys. Rev. Lett.* **82** 3540–3543
- [4] Taniguchi H, Itoh M, and Yagi T 2007 *Phys. Rev. Lett.* **99** 017602
- [5] Bussmann-Holder A and Bishop A R 2006 *Eur. Phys. J. B* **53** 279–282
- [6] Lytle F W 1964 *J. Appl. Phys.* **35** 2212–2215
- [7] Hui Q, Tucker M G, Dove M T, Wells S A, and Keen D A 2005 *J. Phys.: Condens. Matter* **17** S111–S124
- [8] Fischer M, Lahmar A, Maglione M, San Miguel A, Itie J P, and Polian A 1994 *Phys. Rev. B* **49** 12451–12456
- [9] Ravel B and Stern E A 1995 *Physica B* **208/209** 316–318
- [10] Kuzmin A and Purans J 2000 *J. Phys.: Condens. Matter* **12** 1959–1970
- [11] Timoshenko J, Kuzmin A, Purans J 2014 *J. Phys.: Condens. Matter* **26** 055401.
- [12] Rehr J J and Albers R C 2000 *Rev. Mod. Phys.* **72** 621
- [13] Aksenov V L, Kovalchuk M V, Kuzmin A, Purans J, and Tyutyunnikov S I 2006 *Crystallogr. Rep.* **51** 908
- [14] Kuzmin A 1995 *Physica B* **208-209** 175
- [15] Ankudinov A L, Ravel B, Rehr J J and Conradson S D 1998 *Phys. Rev. B* **58** 7565–7576
- [16] Anspoks A, Bocharov D, Purans J, Rocca F, Sarakovskis A, Trepakov V, Dejneka A, and Itoh M 2014 *Phys. Scripta* **89** 044002
- [17] Vedrinskii R V, Kraizman V L, Novakovich A A, Demekhin Ph V, and Urazhdin S V 1998 *J. Phys.: Condens. Mat.* **10** 9561–9580
- [18] Timoshenko J and Kuzmin A 2009 *Comp. Phys. Commun.* **180** 920–925
- [19] Purans J, Affy N D, Dalba G, Grisenti R, De Panfilis S, Kuzmin A, Ozhogin V I, Rocca F, Sanson A, Tiutiunnikov S I, Fornasini P 2008 *Phys. Rev. Lett.* **100** 055901:1-4